



## Full length article

# Schisandrin B prevents ulcerative colitis and colitis-associated-cancer by activating focal adhesion kinase and influence on gut microbiota in an in vivo and in vitro model



Jiani Li<sup>a,1</sup>, Yuan Lu<sup>a,1</sup>, Duowei Wang<sup>a,1</sup>, Fei Quan<sup>a</sup>, Xin Chen<sup>a</sup>, Rui Sun<sup>a</sup>, Sen Zhao<sup>a</sup>, Zhisen Yang<sup>e</sup>, Weiyan Tao<sup>a</sup>, Dong Ding<sup>a</sup>, Xinghua Gao<sup>a</sup>, Qiuhua Cao<sup>a</sup>, Dandan Zhao<sup>a</sup>, Ran Qi<sup>a</sup>, Cheng Chen<sup>c,d</sup>, Lihua He<sup>a</sup>, Kaiyong Hu<sup>a</sup>, Zhen Chen<sup>b,\*\*\*</sup>, Yong Yang<sup>a,\*\*</sup>, Yan Luo<sup>a,\*</sup>

<sup>a</sup> Center for New Drug Safety Evaluation and Research, State Key Laboratory of Natural Medicines, China Pharmaceutical University, Nanjing, 211198, China

<sup>b</sup> Pharmacology Department, China Pharmaceutical University, Nanjing, 211198, China

<sup>c</sup> College of Food Science and Technology, Nanjing Agricultural University, Nanjing, 210095, China

<sup>d</sup> Jiangsu Vocational Institute of Commerce, Nanjing, 211168, China

<sup>e</sup> No.30 Middle School of Taiyuan, Taiyuan, 030002, China

## ARTICLE INFO

## ABSTRACT

## Keywords:

Ulcerative colitis (UC)  
Schisandrin B (SchB)  
Focal adhesion kinase (FAK)  
Colitis-associated cancer (CAC)  
Gut microbiota

Colitis-associated cancer (CAC) has a close relationship with ulcerative colitis (UC). Therapeutic effect of Schisandrin B (SchB) on UC and CAC remains largely unknown. We investigated the preventative effect of SchB on the dextran sulphate sodium (DSS) model of UC and azoxymethane (AOM)/DSS model of CAC. Furthermore, focal adhesion kinase (FAK) activation and influence on commensal microbiota are important for UC treatment. Impact on FAK activation by SchB in UC development was evaluated in vivo and vitro. We also conducted 16S rRNA sequencing to detect regulation of gut microbiota by SchB. Enhanced protection of intestinal epithelial barrier by SchB through activating FAK contributed to protective effect on colon for the fact that protection of SchB can be reversed by inhibition of FAK phosphorylation. Furthermore, influence on gut microbiota by SchB also played a significant role in UC prevention. Our results revealed that SchB was potent to prevent UC by enhancing protection of intestinal epithelial barrier and influence on gut microbiota, which led to inhibition of CAC. SchB was potential to become a new treatment for UC and prevention of CAC.

## 1. Introduction

Colorectal cancer (CRC) is one of the most common cancers worldwide and the third leading cause of cancer mortality in the world (Zeuner et al., 2014). Colitis-associated cancer (CAC), a subtype of CRC, is characterized by chronic inflammation before formation of aberrant crypt foci, polyps, adenomas, and carcinomas (Terzic et al., 2010; Ullman and Itzkowitz, 2011). Inflammatory bowel disease (IBD) is an important risk factor for the development of CAC. Therefore, it is significant to alleviate IBD before it develops to CAC. Ulcerative colitis (UC), which is a subtype of IBD and involves genetic predisposition, epithelial barrier defects, dysregulated immune responses, and environmental factors, has become a worldwide condition (Laharie, 2017;

Ungaro et al., 2017).

A large number of factors participate in equilibrium of intestinal epithelial barrier, among which Focal adhesion kinase (FAK) is one of the most important factors (Leoni et al., 2013). FAK is a cytoplasmic protein tyrosine kinase which regulates cell motility, proliferation and survival in kinase dependent or independent mechanism (Sulzmaier et al., 2014). It has been reported that FAK plays an important role in maintaining homeostasis of tight junctions (Wang et al., 2011; Yamada et al., 2005) in blood-testis barrier (Siu et al., 2009; Su et al., 2011) and intestine (Guo et al., 2015). Previous study has demonstrated that intestinal epithelium (IE)-specific conditional FAK knockout mice were profoundly more susceptible to DSS-induced colitis than wide type littermates (Owen et al., 2011) and that FAK was required for intestinal

\* Corresponding author.

\*\* Corresponding author.

\*\*\* Corresponding author.

E-mail addresses: [cj@cpu.edu.cn](mailto:cj@cpu.edu.cn) (Z. Chen), [yy@cpu.edu.cn](mailto:yy@cpu.edu.cn) (Y. Yang), [1620164337@cpu.edu.cn](mailto:1620164337@cpu.edu.cn) (Y. Luo).

<sup>1</sup> These authors contributed equally to the present study.

regeneration downstream of Wnt/c-Myc Signaling (Ashton et al., 2010). Therefore, FAK is a potential target to promote regeneration of intestinal epithelium after damage but the underlying mechanism remains elusive.

Emerging evidence supports a pivotal role for the microbiota in the modulation of homeostasis of host immune activation (Owen and Mohamadzadeh, 2013; Slater et al., 2017; Tsoi et al., 2017), although the underlying mechanism needs to be elucidated (Chu et al., 2016; Garrett, 2015; Ijssennagger et al., 2015). Abnormality of host-microbiota interactions plays an important role in development of many diseases, including CAC and IBD (Chiari et al., 2017; Forbes et al., 2016; Gagniere et al., 2016; Yamamoto and Matsumoto, 2016; Yang et al., 2013). It is also notable that transfer of whole microbiota via fecal transplantation has already been shown to ameliorate the severity of diseases, including UC (Hudson et al., 2017). Gut microbiota seems to be a potential target for treatment of UC and CRC, but the efficiency of regulating gut microbiota together with other treatments needs to be further evaluated.

Schisandrin B (SchB) is one of the most abundant bioactive dibenzocyclooctadiene derivatives found in the fruit of Schisandra chinensis. It can alleviate a wide range of diseases such as hepatitis, doxorubicin-induced cardiotoxicities and cancer metastasis (Checker et al., 2012; Kwan et al., 2015; Lam and Ko, 2012; Li et al., 2006, 2007; Nishida et al., 2009; Pan et al., 2006; Qiangrong et al., 2005; Sun et al., 2007; Zhang et al., 2013). However, little is known about the effects of SchB for UC and CAC and if so, the underlying mechanism remains largely elusive.

Here we demonstrated that SchB effectively prevented initiation and promotion of DSS-induced UC. We also found that SchB significantly reduced intestine epithelium permeability and protected tight junctions in DSS-treated mice. Later we revealed that SchB protected colon by activating FAK and downstream signaling and influence on gut microbiota. Finally, we tested if SchB prevented initiation of AOM/DSS-induced CAC. Notably, we revealed the underlying mechanism how SchB alleviated DSS-induced UC and AOM/DSS-induced CAC in mice and found a natural compound which potentially becomes a new prevention and treatment of CAC and UC.

## 2. Materials and methods

### 2.1. Statistical analysis

Adobe Illustrator CC was used to create the graphic artwork. Statistical analysis was performed using the GraphPad Prism software (GraphPad Prism Software, Version 7.0a, GraphPad, San Diego, CA) and SPSS for Windows 15.0.0 (SPSS, Inc., USA) statistical software. For comparisons, a one-way analysis of variance and Student's t-tests (two-tailed) were performed as appropriate except Figs. 5 and 6. Data in these graphs did not follow a normal distribution, for these data a nonparametric test such as the Mann-Whitney U test was used. Survival curves were estimated using the Log-rank method. Statistically significant differences are shown with asterisks as follows: \*P < 0.05, \*\*P < 0.01, \*\*\*P < 0.001 and \*\*\*\*P < 0.0001; whereas, ns indicates comparisons that are not significant.

### 2.2. Mice and reagents

All mice used in this work were C57BL/6 male mice. All C57BL/6 male mice were purchased from Beijing Vital River Laboratory Animal Technology Co., Ltd. All mice were bred and maintained in Center for New Drug Safety Evaluation and Research in China Pharmaceutical University. All animal experiments were conducted in accordance with the National Institutes of Health Guide for the Care and Use of Laboratory Animals with the approval of the Animal Ethics Committee of China Pharmaceutical University (Nanjing, China). DSS treatment to induce UC and AOM/DSS treatment to induce colon adenocarcinoma

are as previous described (Gao et al., 2018). Briefly, for acute DSS colitis inducement, mice were exposed to DSS (36–50 kDa, MP Biomedicals) concentration of 2.5% (w/v) in the drinking water for 7 days. As for AOM/DSS model, mice were injected with AOM working solution (10 mg per kg body weight, i.e., 100 µl working solution per 10 g mouse body weight) intraperitoneally for the experimental group or sterile isotonic saline for the control group. The mice were treated with DSS (water only for control groups) concentration of 2.5% (w/v) in the drinking water for consecutive 7 days, beginning from 7 days after AOM injection. Consecutive DSS treatment was repeated for 2 cycles every 3 weeks (Fig. 7A). SchB, which was administrated by gavage, were dissolved in 0.5% sodium carboxymethyl cellulose (CMC-Na, Sinopharm) at dose of 15 mg/kg and 30 mg/kg and corresponding vehicle was 0.5% CMC-Na. For PF562271 treatment, PF562271 was dissolved in 0.5% CMC-Na at the dose of 50 mg/kg and given to the mice twice a day by gavage. SchB (purity 98.0%) was purchased from the National Institutes for Food and Drug Control (Beijing, China).

### 2.3. Disease activity index, liver index and spleen index evaluation

Disease activity index evaluation was previously described. The disease activity index = (combined score of weight loss, stool consistency and bleeding)/3. Criteria were the same as those in the article *Therapeutic effect of intracolonically administered nuclear factor kappa B (p65) antisense oligonucleotide on mouse dextran sulphate sodium (DSS)-induced colitis* (Murano M et al.) (Murano et al., 2000). Liver index is the ratio of liver weight to body weight (mg/g) (Zheng et al., 2009). Spleen index is the ratio of spleen weight to body weight as previously described (mg/g) (Chen et al., 2013).

### 2.4. Immunohistochemistry

Colon tissues were fixed with 4% paraformaldehyde and sectioned into 3-µm -thick slide. Slides were heated in a microwave submersed in 1 × citrate unmasking solution until boiling was initiated, followed by 20 min at sub-boiling temperature (95°C–98 °C). Slides were cooled in room temperature for 30 min. Colon tissue slides were permeabilized with 0.3% Triton X-100 in phosphate buffered saline, pH 7.4 (PBS). Samples were blocked with 10% goat serum (Solarbio, SL038) and incubated with primary antibody at 4 °C overnight. The antibodies were shown in Table 1. MaxVision TM HRP-Polymer anti-rabbit IHC Kit (MAX biotechnologies, KIT-5004) was used for HRP label. DAB kit (MAX biotechnologies, DAB-0031) was used for detection.

### 2.5. In vivo permeability assay

Intestinal permeability was detected by in vivo FITC-dextran (Sigma-Aldrich) permeability assay as described previously (Sommer et al., 2014). Mice were fasted for 4 h, followed by being gavaged with 0.6 mg/g body weight FITC-dextran (4 KDa) solution and blood was collected by orbital bleeding after 3 h. Fluorescence intensity in the plasma was measured using Fluorescence Spectrophotometer (EnSpire, 2300). FITC-dextran concentrations were determined from a standard curve generated by serial dilutions of FITC-dextran.

### 2.6. Cell culture

Human intestinal epithelium cell lines CACO2 and HCT116 were purchased from the Shanghai Cell Collection (Chinese Academy of Sciences, Shanghai, China). iBMDM cell line is stored in China Pharmaceutical University. CACO2 and HCT116 cell lines were cultured in DMEM growth media supplemented with 10% FBS (Biological Industries, Israel) and were maintained at 37 °C in a fully humidified atmosphere of 5% CO<sub>2</sub>. SchB was dissolved in DMSO at concentration of 100 mM to make stock solution, which was diluted to 6.25 µM and 12.5 µM, respectively.

**Table 1**  
Antibodies used in this study.

Antibody	Manufacture	Catalog number	Application
anti-FAK (phospho-Y397) antibody	abcam	ab81298	Immunohistochemistry
anti-Occludin antibody	abcam	ab168986	Immunohistochemistry
anti-Ki67 antibody	CST	12202	Immunohistochemistry
Anti-CD45-Apc-cy7	eBioscience	103116	Flow cytometry
Anti-CD11b-BV510	eBioscience	101263	Flow cytometry
Anti-F4/80-APC	eBioscience	17-4801-82	Flow cytometry
Anti-Ly6G-PE-cy7	eBioscience	127618	Flow cytometry
phospho-FAK (Tyr397) antibody	CST	#3283	Western blot
FAK antibody	CST	#3285	Western blot
p-p38/MAPK antibody	CST	#4511	Western blot
p38/MAPK antibody	CST	#8690	Western blot
E-cadherin antibody	Wanleibio	WL01482	Western blot
phospho-SAPK/JNK (Thr183/Tyr185) (81E11) Rabbit mAb	CST	#9252	Western blot
JNK antibody	CST	#4060	Western blot
p-Akt antibody	CST	#4691	Western blot
Akt antibody	CST	#4370	Western blot
p-Erk antibody	CST	#4695	Western blot
Erk antibody	CST	#AC251	Western blot
CDK4 antibody	Beyotime	#AC256	Western blot
CDK6 antibody	Beyotime	#6078-1-Ig	Western blot
Bcl2 antibody	Proteintech		

CST stands for cell signaling technology.

For preparing of primary bone marrow derived macrophages, we conducted the experiments as previously described (Na et al., 2015; Weischenfeldt and Porse, 2008). Briefly, we separated the cells from the bone marrow and added M-CSF (10 ng/ml) (Peprotech, 315-02) into the medium. After 7 days of differentiation, we stimulated the cells with lipopolysaccharide (LPS) and treated them with SchB.

## 2.7. ELISA assays

To measure the release of inflammatory cytokines, ELISA was conducted using colon lysate of mice and media from BMMDM and iBMMDM cells challenged with LPS. ELISA was performed using ELISA kits for detecting of mouse/human interleukin-6 (m/h IL-6), mouse/human tumor necrosis factor- $\alpha$  (m/h TNF- $\alpha$ ), mouse/human interleukin-1 $\beta$  (m/h IL-1 $\beta$ ) (Dakewe Biotech Co., Ltd.) on a 96-well Nunc immune plate according to the manufacturer's protocol. After terminating the reaction with a stop solution, the absorbent intensity was detected using a spectrophotometer at a wavelength of 450 nm.

## 2.8. Extraction of immune cells in colonic lamina propria of mice and flow cytometry analysis

Isolation of colonic lamina propria cells was performed following a previously established method (Gao et al., 2018). In brief, luminal content and fat tissue were removed and colons were cut into 0.5 cm pieces, followed by washing with ice-cold PBS. Colons were first incubated with HBSS (without Ca $^{2+}$  and Mg $^{2+}$ ) containing 5% FBS, 2 mM EDTA, and 1 mM DTT to remove epithelial cells and mucus, and then digested in PBS solution containing 5% FBS, 1 mg/ml collagenase VIII (Sigma), and 0.1 mg/ml DNase I (Roche). Digested cell suspension was washed with PBS solution and filtered with a 45- $\mu$ m cell strainer. Antibodies were shown in Table 1. Cells were analyzed with MACS-Quant Analyzer 10 (Miltenyi Biotec). Flow cytometry analysis was done with FlowJo software.

## 2.9. Protein extraction and quantification

Protein of colon tissue and cells was extracted using protein lysis buffer containing 200 mM NaCl, 20 mM Tris, 10% glycerinum, 0.3 mM EDTA, 1% Triton X-100, 10 mM NaF, 10 mM Na $_3$ VO $_4$ , 20 mM  $\beta$ -Sodium 3-phosphoglycerate, 5 mM Na $_4$ P $_2$ O $_7$ , 1 mM PMSF and 10 mM EDTA-free Protease Inhibitor Cocktail (Roche). Protein quantification was carried out using Pierce™ BCA Protein Assay Kit (Thermo Scientific, 23225). The absorbent intensity was detected using a spectrophotometer at a wavelength of 570 nm.

## 2.10. Western blot

Protein samples (15–20  $\mu$ g) were electrophoresed on an 10%–15% (variation due to the molecular weight of the protein) SDS-polyacrylamide gel and transferred onto a polyvinylidene difluoride (PVDF) membrane (Millipore, USA). After blocking with 5% BSA (Bovine Serum Albumin, Sigma) for 1 h at room temperature, the membranes were incubated with primary antibody overnight at 4 °C. Primary antibodies were shown in Table 1. After being washed with TBST buffer, the membranes were incubated with horseradish peroxidase (HRP)-conjugated secondary antibody (goat anti-rabbit/mouse IgG-HRP, Santa Cruz Biotechnology, USA) for 2 h at room temperature. The bands were visualized using an ECL (CWbio, CW0048, China) detection system. The expression of  $\beta$ -actin (Proteintech, China) was used as a control.

## 2.11. RNA isolation and cDNA synthesis

Total RNA was extracted from 50 to 100 mg of colon tissues using RNAiso Plus reagent (Takara Bio, Japan) according to the manufacturer's instructions. RNA concentration and purity was measured using the Micro Spectrophotometer (KAIAO, K5500) and the integrity was confirmed using 1.2% agarose gel (Gene Tech, Shanghai, China). As for cDNA synthesis, PrimeScript™ RT reagent Kit with gDNA Eraser (Perfect Real Time), the residue of genomic DNA was removed in a volume of 10  $\mu$ l at 42 °C for 2 min, containing 1.5  $\mu$ g of RNA samples, 2  $\mu$ l 5  $\times$  gDNA Eraser Buffer, 1  $\mu$ l gDNA Eraser and RNase Free dH $_2$ O. Immediately after this, first strand cDNA synthesis was performed by adding 4  $\mu$ l of 5  $\times$  PrimeScript Buffer, 1  $\mu$ l of PrimerScript RT Enzyme Mix, 1  $\mu$ l of RT Enzyme and 4  $\mu$ l RNase Free dH $_2$ O at 37 °C for 15 min, 85 °C for 15 s.

## 2.12. Gene expression analysis by realtime-PCR(RT-PCR)

Realtime-PCR was performed using the PrimeScript™ RT reagent Kit (Takara, RR037A). Reactions were run on the ABI StepOnePlus (ABI, USA). Relative changes in mRNA and expression were determined using the  $2^{-\Delta\Delta Ct}$  method for mIL-6, TNF- $\alpha$ , mIL-1 $\beta$ , mIL-12, mIL-23, and mLgr5. The sequences of the PCR primers (forward and reverse, respectively) are 5'-CAATGGACAGAAATATCAAC-3' and 5'-ACAGGACAG GTATAGATT-3' for mIL-1 $\beta$ ; 5'-TTCTGTCTACTGAACCTTC-3' and 5'-CCATAGAACCTGATGAGAG-3' for TNF- $\alpha$ ; 5'-CTGCAAGAGACTTCCA TCCAG-3' and 5'-AGTGGTATAGACAGGTCTGTTGG-3' for mIL-6; 5'-ACATCTGCTCTCCACAAG-3' and 5'-GGTGCTTCACACTTCAG GAA-3' for mIL-12; 5'-ACCACACCTTCTACAATGAG-3' and 5'-ACGACC AGAGGCATACAG-3' for mActin; 5'-AGTAATAATGCTATGGCTGTTG-3' and 5'-TCATCCTCTCTTAGTAG-3' for mIL-23; 5'-CCTGAACTA AGAACACTGAC-3' and 5'-GCACCTGGAGATTAGGTAAC-3' for mLgr5. The expression of mActin was used as a control.

## 2.13. Compositional analysis of the gut microbiota by pyrosequencing and data analysis

Sample collection and compositional analysis of the gut microbiota were conducted as previously described (Caporaso et al., 2011; Gao

et al., 2018). Colon content homogenates in PBS were immediately frozen ( $-80^{\circ}\text{C}$ ) and stored until further processing. Next generation sequencing library preparations and Illumina MiSeq sequencing were conducted at GENEWIZ, Inc. (Suzhou, China). In brief, 30–50 ng DNA was used to generate amplicons using a MetaVx™ Library Preparation kit (GENEWIZ, Inc., South Plainfield, NJ, USA). The QIIME data analysis package was used for 16S rRNA data demultiplexed, quality filtered and data analysis. For normalization of the sequencing data, rarefaction was used. Sequence were grouped into operational taxonomic units (OTUs) using the clustering program VSEARCH (1.9.6) against the Silva 119 database pre-clustered at 97% sequence identity. For alpha diversity, Chao1 and Shannon index was used to characterize  $\alpha$  diversity in a community. Beta diversity was calculated using weighted and unweighted UniFrac and principal coordinate analysis (PCoA) was performed. ANOSIM analysis was conducted using vegan R package.

### 3. Results

#### 3.1. SchB potently inhibits initiation and promotion of UC

The connection between colitis and CAC was well-established in the last decade. Because DSS-induced inflammation is indispensable and pivotal in AOM/DSS-induced CAC, we first investigated if SchB could alleviate DSS-induced UC. We conducted the experiment as shown in Fig. 1A. SchB slightly reversed body weight loss of DSS-induced colitis mice at 15 mg/kg and 30 mg/kg dose (Fig. 1B). SchB was also competent to recover decrease of colon length and diminish disease activity index of DSS-treated mice at 15 mg/kg and 30 mg/kg dose (Fig. 1C and D). However, SchB did not significantly change liver index and spleen index of control mice and DSS-treated mice (Fig. S1A and S1B). Furthermore, histopathology section showed that DSS mainly damaged distal colon rather than proximal colon. SchB-treated mice, especially at 30 mg/kg dose, suffered less severe UC for shorter damaged area, less submucosa edema and more integrated intestinal epithelium (Fig. 1E). Immunohistochemical staining analysis also revealed that Ki67, the marker of proliferate cells, was significantly downregulated in DSS-treated mice, compared to control mice. SchB could significantly upregulate expression of Ki67 (Fig. S2A and Fig. S2B). As shown in Fig. S2C, DSS exposure strongly inhibited CDK4/CDK6, the most important cell cycle promoting kinase and Bcl2, one of the key apoptosis inhibitors. However, SchB could restore the expression of CDK4/CDK6 and Bcl2 in a dose dependent manner (Fig. S2C-S2F). q-PCR analysis revealed that Lgr5, one of the important regeneration related genes, decreased in DSS-treated mice and was restored by SchB (Fig. S2G). Notably, SchB alone did not cause any intestine damage in intestine of normal mice (Fig. 1B, 1D, 1E, 1F, S1A and S1B). The mRNA and protein levels of murine interleukin-6 (mIL-6), tumor necrosis factor  $\alpha$  (TNF- $\alpha$ ) and murine interleukin-1 $\beta$  (mIL-1 $\beta$ ) decreased in the colon of mice in DSS + SchB (15 mg/kg) and DSS + SchB (30 mg/kg) groups compared to those in DSS + vehicle group (Fig. 1G-L). Expression of murine interleukin-12 (mIL-12) and murine interleukin-23 (mIL-23) were also diminished by SchB (Fig. S2H and S2I). At last, we measured inflammatory cell infiltration in colonic lamina propria by flow cytometry. The most important inflammatory cells involved in DSS-induced colitis were macrophage and neutrophil (Chassaing et al., 2014). As shown in Fig. S3, both CD45 $^{+}$ CD11b $^{+}$ F4/80 $^{+}$  macrophage and CD45 $^{+}$ CD11b $^{+}$ Ly6G $^{+}$  neutrophil could be recruited in colon by DSS exposure and diminished by SchB treatment, both at low (15 mg/kg) and high dose (30 mg/kg). These results indicated that SchB potently inhibited initiation and promotion of UC.

#### 3.2. SchB exhibits protective effect on intestinal epithelial barrier in DSS-induced model

UC is a multifactorial disease in which immune response, epithelial

barrier integrity and host-microbiota interaction are involved (Laharie, 2017). Firstly, we investigated if SchB ameliorated DSS-induced UC by inhibition of immune system. It has been reported that innate immune cells, including macrophages, play a fundamental role in DSS-induced UC (Chassaing et al., 2014). Therefore, we tested if SchB could influence function of macrophages in vitro. SchB failed to reduce Lipopolysaccharide (LPS)-induced TNF- $\alpha$  and mIL-6 release in Primary Bone Marrow Derived Macrophages (BMDM) (Fig. S4A and S4C) and immortalized Bone Marrow Derived Macrophage (iBMDM) cell lines (Fig. S4B and S4D). Furthermore, LPS-induced sepsis model, in which innate immune cells activation plays a fundamental role, was conducted to evaluate if SchB has immunosuppression function. As a result, SchB could not improve survival of LPS-treated mice, even the dose reached to 300 mg/kg (Fig. S4E and S4F). Therefore, SchB alleviated UC by other mechanisms apart from suppressing innate immune cells.

Later, we investigated if SchB protected intestinal epithelial barrier. In vivo FITC-dextran permeability assay revealed that dextran flux significantly increased in DSS-treated mice compared to normal mice and SchB could potently decreased dextran flux in DSS-treated mice (Fig. 2A), indicating that SchB was responsible for protecting intestinal epithelial barrier function. Expression and distribution of tight junction protein (TJ protein) were determined by western blot and immunohistochemical staining. E-cadherin, one of the most important TJ proteins, significantly decreased in DSS-treated mice, and SchB distinctly increased E-cadherin level in colon of DSS-treated mice, at both 15 mg/kg and 30 mg/kg dose (Fig. 2B and C). Immunohistochemical staining assay and western blot revealed that Occludin, another significant TJ protein, was mainly expressed in gut mucosa and epithelial cells. DSS-treated mice showed damaged colon mucosa and lower expression level of Occludin compared to normal mice and SchB could distinctly restore the expression of Occludin (Fig. 2B, D and 2E). These data indicated that SchB protected intestinal epithelial barrier.

#### 3.3. SchB protects intestinal epithelial barrier by activating FAK both in vivo and *in vitro*

FAK is a multifunctional regulator of many biological processes such as cell mobility, proliferation and restoration (Sulzmaier et al., 2014). It is possible that FAK is related to survival of colon epithelial cells. We suspected that FAK activation is indispensable for colon protection. Immunohistochemistry analysis manifested that phosphorylation-FAK (Tyr 397) mainly distributed in colon mucosa, especially in epithelial cell (Fig. 3A). The phosphorylation-FAK (Tyr 397) expression was dampened on colon in DSS-treated mice, and SchB recovered phosphorylation-FAK expression in epithelial cell (Fig. 3A). Western Blot analysis revealed that phosphorylation-FAK (Tyr 397) is diminished in colon of DSS-treated mice and SchB significantly increased the expression of phosphorylation-FAK (Tyr 397) (Fig. 3B). SchB-treated colitis mice not only suffered less severe colon damage, but also expressed higher level of phosphorylation-FAK. These data indicated that activation of FAK related to more modest colon damage. To further evaluate if FAK activation is indispensable for protective effect of SchB, we used PF562271, a potent, ATP-competitive and reversible inhibitor of FAK, to test if phosphorylation-FAK inhibition could reverse colon protection of SchB. HE staining analysis substantiated that PF562271 alone did not cause intestinal epithelium damage (Fig. 3E). However, when treated with both PF562271 and DSS, the mice exhibited longer damaged area and more serious colonic mucosa damage than treated with DSS alone, which manifested that activation of FAK could partly enhance repair of intestinal epithelium. HE staining analysis, colon length (Fig. 3C) and disease activity index (Fig. 3D) verified that PF562271 could reverse colon protective effect of SchB. Furthermore, immunohistochemistry experiment also showed that PF562271 alone did not reduce Occludin expression in colonic mucosa but it can counteract increasing of Occludin expression by SchB (Fig. 3F). Therefore, SchB failed to protect colon from DSS-induced damage at the presence of PF562271, which

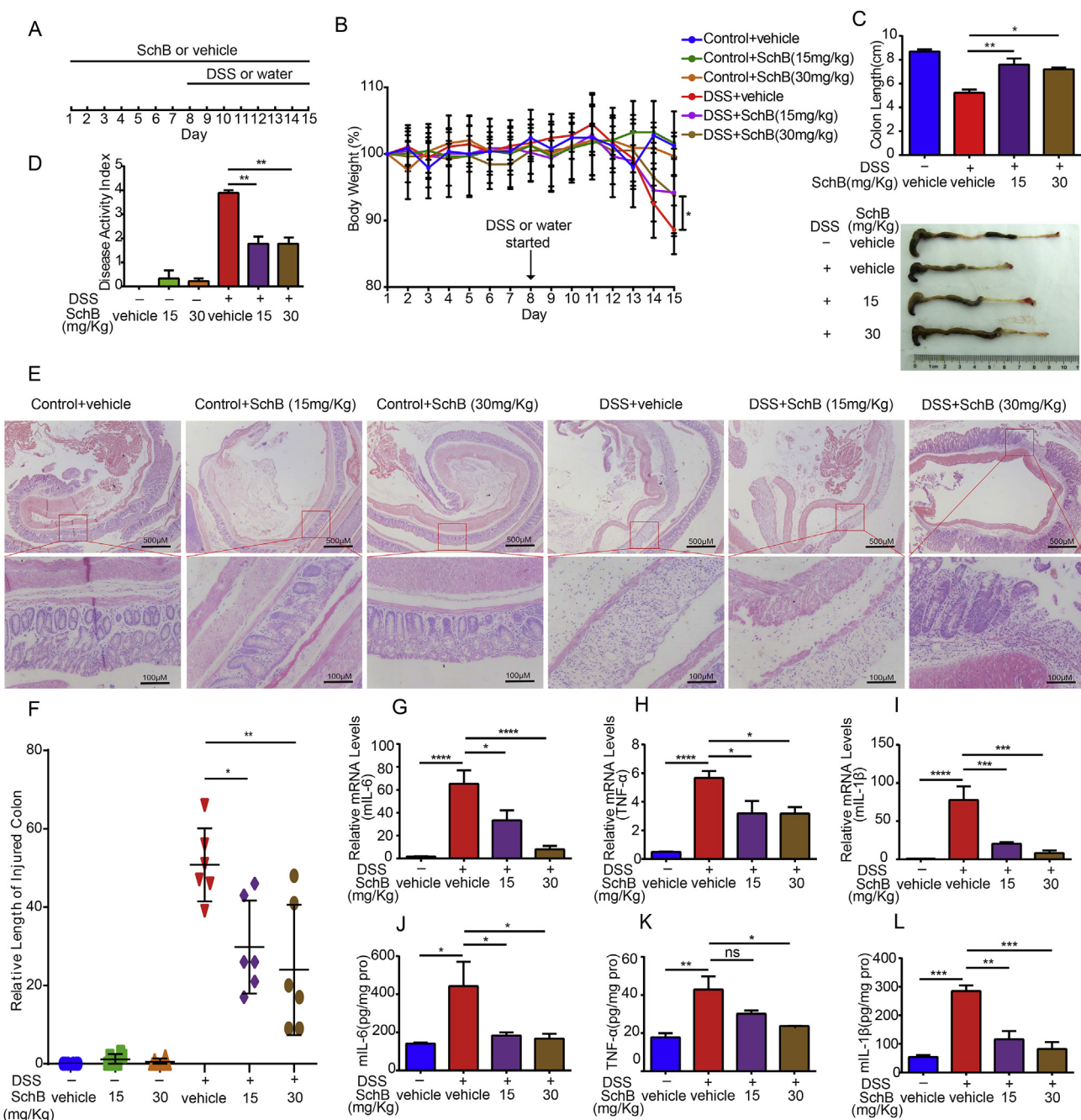


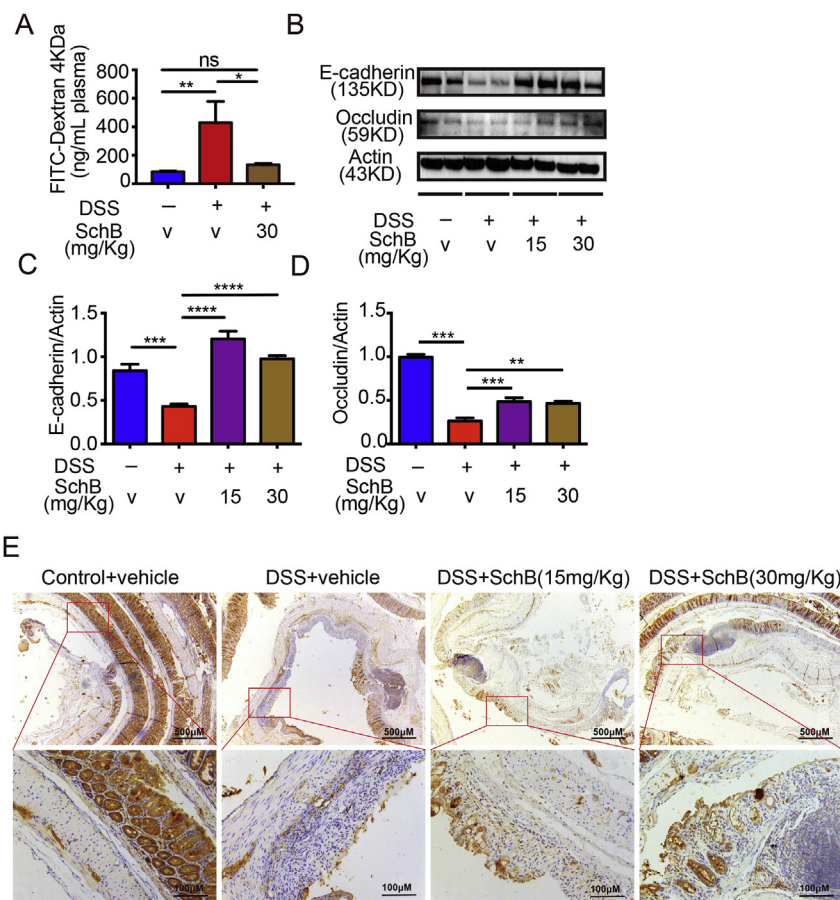
**Fig. 1.** SchB significantly prevents initiation and progression of UC. For DSS model, the groups are as follows: Control + vehicle, Control + SchB (15 mg/kg), Control + SchB (30 mg/kg), DSS + vehicle, DSS + SchB (15 mg/kg), DSS + SchB (30 mg/kg). Vehicle was 0.5% CMC-Na. Concentration of DSS was 2.5% (w/v) in drinking water. (A) Procedure of DSS-induced acute colitis model induction and SchB treatment, n = 6. (B) Body weight change of normal or DSS challenged mice treated with SchB at indicated doses in the corresponding figure (0.5% CMC-Na for vehicle). n = 6. (C) Colon length and (D) Disease activity index of DSS-induced UC mice treated with SchB at indicated doses in the corresponding figure (0.5% CMC-Na). n = 6 (E) H&E staining of normal or DSS challenged mice treated with SchB at indicated doses in the corresponding figure (0.5% CMC-Na for vehicle). Scale bars, 500  $\mu$ M for upper lines and 100  $\mu$ M for lower lines. (F) Relative lengths of damaged colon calculated using image J software. n = 6. (G–I) Relative mRNA levels in mice colon (Fig. 1G) for murine IL-6 (mIL-6), 1H for murine TNF- $\alpha$  (mTNF- $\alpha$ ), and 11 for murine IL-1 $\beta$  (mIL-1 $\beta$ ). (J–L) ELISA assessing for cytokines levels in mice colon (Fig. 1J) for murine IL-6 (mIL-6), 1K for murine TNF- $\alpha$  (mTNF- $\alpha$ ), and 1L for murine IL-1 $\beta$  (mIL-1 $\beta$ ). Data were presented as the mean  $\pm$  S.E.M. \*P < 0.05, \*\*P < 0.01, \*\*\*P < 0.001 and \*\*\*\*P < 0.0001 vs. Control + vehicle group or DSS + vehicle group. Scale bars are showed in figures.

indicated that FAK activation was essential for protective effect of SchB.

#### 3.4. SchB stimulates activity of downstream signal of FAK both in vitro and vivo

To further verify if FAK associated signaling was activated in vitro and vivo, we assessed if FAK downstream kinase was phosphorylated.

Since it has been reported that activation of FAK is related to an increased expression of p-JNK, p-p38/MAPK, p-Akt and p-Erk (Cui et al., 2017; Shi et al., 2016), which are involved in mobility and survival of epithelial cells, we suspected that SchB could stimulate FAK associated signaling in intestinal epithelial cells. Treated with SchB at 6.25  $\mu$ M and 12.5  $\mu$ M for 2 h, both CACO2 and HCT116 expressed higher levels of p-FAK (Y397) in a dose-dependent manner (Fig. 4A, 4B, 4G and 4H).



However, SchB treatment for 4 h did not have that distinct effect as for 2 h (Fig. S5A and S5B). We also measured phosphorylation of JNK (Thr183/Tyr185), p38/MAPK (Thr180/Tyr18), Akt (Ser473) and Erk (Thr202/Tyr204). Notably, downstream of FAK was also stimulated by SchB (12.5 µM) treatment for 2 h (Fig. 4A, 4C-4F, 4G and 4I-4K). SchB at the dose of 6.25 µM significantly increased expression of phosphorylation of JNK (p-JNK), p38/MAPK (p-p38/MAPK) and Erk (p-Erk) in CACO2 cell line, as well as p-JNK in HCT116 cell line. These data suggested that SchB stimulated activity of downstream signal of FAK in intestinal epithelial cells. At last, we confirmed these results in mice colon tissues. As shown in Fig. 4L-P, p-JNK, p-p38/MAPK, p-Akt and p-Erk were significantly decreased in DSS-treated mice compared to normal mice, and were restored to some extent in SchB-treated mice (Fig. 4L-P). Although phosphorylation of JNK, p38/MAPK and Akt did not exhibit significant increase in DSS + SchB (15 mg/kg) group, however, expression level of p-JNK, p-p38/MAPK, p-Akt and p-Erk significantly increased in DSS + SchB (30 mg/kg) group (Fig. 4L-P), which indicated certain protective effect of SchB on colon.

### 3.5. SchB influences gut microbiota to help inhibiting initiation and promotion of UC

Host-microbiota relationship also plays an important role in development of UC. Microbiota composition influences inflammation response and epithelium barrier function (Chassaing et al., 2015; Gagniere et al., 2016). To investigate if colon protective effect of SchB is, at least in part, due to regulation of microbiota composition, we documented 16S rRNA sequencing to detect the influence of SchB on microbiota composition. First of all, we investigated  $\alpha$  diversity in Control + Vehicle, Control + SchB, DSS + Vehicle and DSS + SchB group. Both Chao1 and Shannon index did not change significantly in four groups, indicating that DSS exposure and SchB treatment could not

**Fig. 2. SchB protects intestinal epithelial barrier and integration of tight junctions of colon.** (A) Intestinal permeability to FITC-dextran in colon tissues. V stands for vehicle. Dose of SchB was 30 mg/kg n = 5 mice per group. (B) Western Blot of E-cadherin and Occludin in mice colon tissues. (C) Quantification of western blot of E-cadherin. (D) Quantification of western blot of Occludin. (E) Immunohistochemistry staining of Occludin in mice colon tissues. Scale bars, 500 µM for upper lines and 100 µM for lower lines. Data were presented as the mean  $\pm$  S.E.M. \*P < 0.05, \*\*P < 0.01, \*\*\*P < 0.001 and \*\*\*\*P < 0.0001 vs. Control + vehicle or DSS + vehicle group.

alter OTU number of gut microbiota (Fig. 5A). Principal Co-ordinates Analysis (PCoA) and ANOSIM analysis revealed that SchB treatment induced slight change in normal mice microbiota, but caused distinct intestinal microbial landscape in DSS-treated mice (Fig. 5B). DSS treatment caused increase of several operational taxonomic units (OTUs) which are reported to correlate with inflammation disorder, such as OTU5 (Fig. 5C), OTU8 (Fig. 5D), OTU66 (Fig. 5E) (Nagalingam et al., 2011), and bloom in OTUs which closely related to colon adenocarcinoma progression, for example OTU219 (Fig. 5F) (Surana and Kasper, 2017). SchB (30 mg/kg) almost eliminated these OTUs in DSS-treated mice. As for other OTUs, which almost disappeared in DSS-treated mice, such as OTU53 (Fig. 5G), OTU23 (Fig. 5H), OTU55 (Fig. 5I) and OTU161 (Fig. 5J), all of them were restored by SchB. Thus, colon protection by SchB was probably associated with regulation of eubiosis of the microbiota composition, least in part.

To further investigate if regulation of microbiota composition contributed to protective effect of SchB, we co-housed the DSS-treated mice which received vehicle or SchB to test if the protection effect of SchB could be counteracted by gut microbiota transmission. As previous data, SchB, at both 15 mg/kg and 30 mg/kg, significantly protected the intestinal epithelial barrier integrity of separately housed colitis mice, according to HE staining analysis (Fig. 6A-D), colon length (Fig. 6I) and disease activity index (Fig. 6J). However, SchB at 15 mg/kg and 30 mg/kg failed to prevent DSS-induced distal colon damage when the DSS-induced colitis mice which received vehicle or SchB were co-housed, which was revealed by HE staining analysis (Fig. 6E-H), colon length (Fig. 6I) and disease activity index (Fig. 6J). Also, SchB did not change liver index and spleen index of the DSS-treated mice, both when separately housed or cohoused, which also indicated that SchB hardly regulated systematic immune response (Fig. 6K and 6L). 16S rRNA sequencing verified that the microbiota transmission eliminated the efficiency of SchB. PCoA analysis showed that microbiota transmission

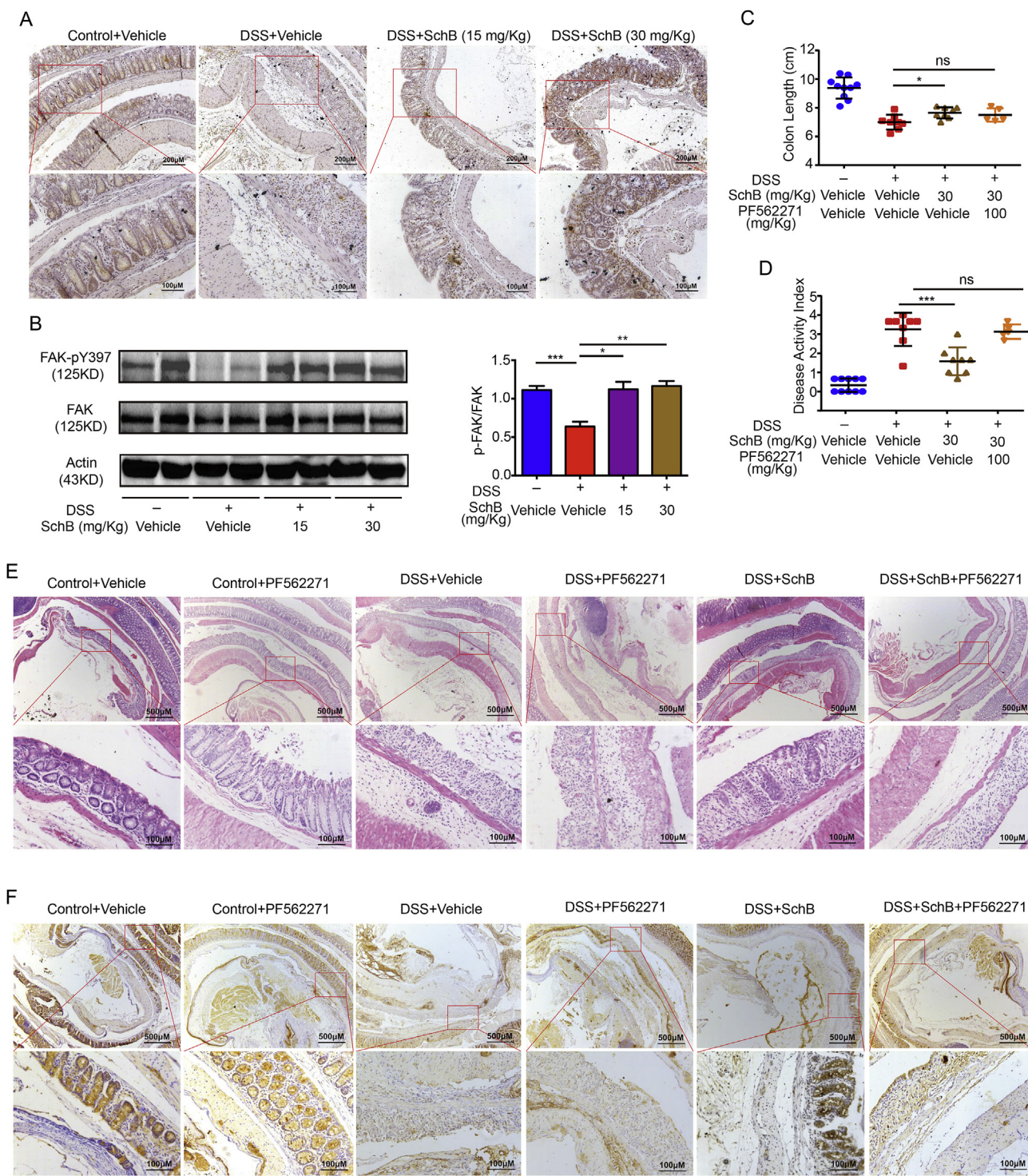


**Fig. 3. SchB protects intestine epithelial barrier of colon by activating FAK.** (A) Immunohistochemistry staining of p-FAK (pY397) in mice colon tissues. (B) Western Blot of p-FAK (pY397) and FAK expression in mice colon tissues. (C) Colon lengths of mice in Control + vehicle, DSS + vehicle, DSS + SchB and DSS + SchB + PF562271 groups. Dose of SchB was 30 mg/kg. Dose of PF562271 was 50 mg/kg, twice a day. (D) Disease Activity index of mice in Control + vehicle, DSS + vehicle, DSS + SchB and DSS + SchB + PF562271 groups. Dose of SchB was 30 mg/kg. Dose of PF562271 was 50 mg/kg, twice a day. (E) H&E staining of colons of mice in Control + Vehicle, Control + PF562271, DSS + Vehicle, DSS + PF562271, DSS + SchB, and DSS + SchB + PF562271 groups. Dose of SchB was 30 mg/kg. Dose of PF562271 was 50 mg/kg, twice a day. (F) Immunohistochemistry staining of Occludin of mice in Control + Vehicle, Control + PF562271, DSS + Vehicle, DSS + PF562271, DSS + SchB, and DSS + SchB + PF562271 groups. Dose of SchB was 30 mg/kg. Dose of PF562271 was 50 mg/kg, twice a day. Data were presented as the mean  $\pm$  S.E.M. \*P < 0.05, \*\*P < 0.01, \*\*\*P < 0.001 and \*\*\*\*P < 0.0001 vs. DSS + vehicle group. For Fig. 3A, scale bars, 200  $\mu$ M for upper lines and 100  $\mu$ M for lower lines. n = 10 mice in Control + Vehicle, DSS + Vehicle and DSS + SchB groups. n = 5 mice in Control + PF562271, DSS + PF562271 and DSS + SchB + PF562271 groups.

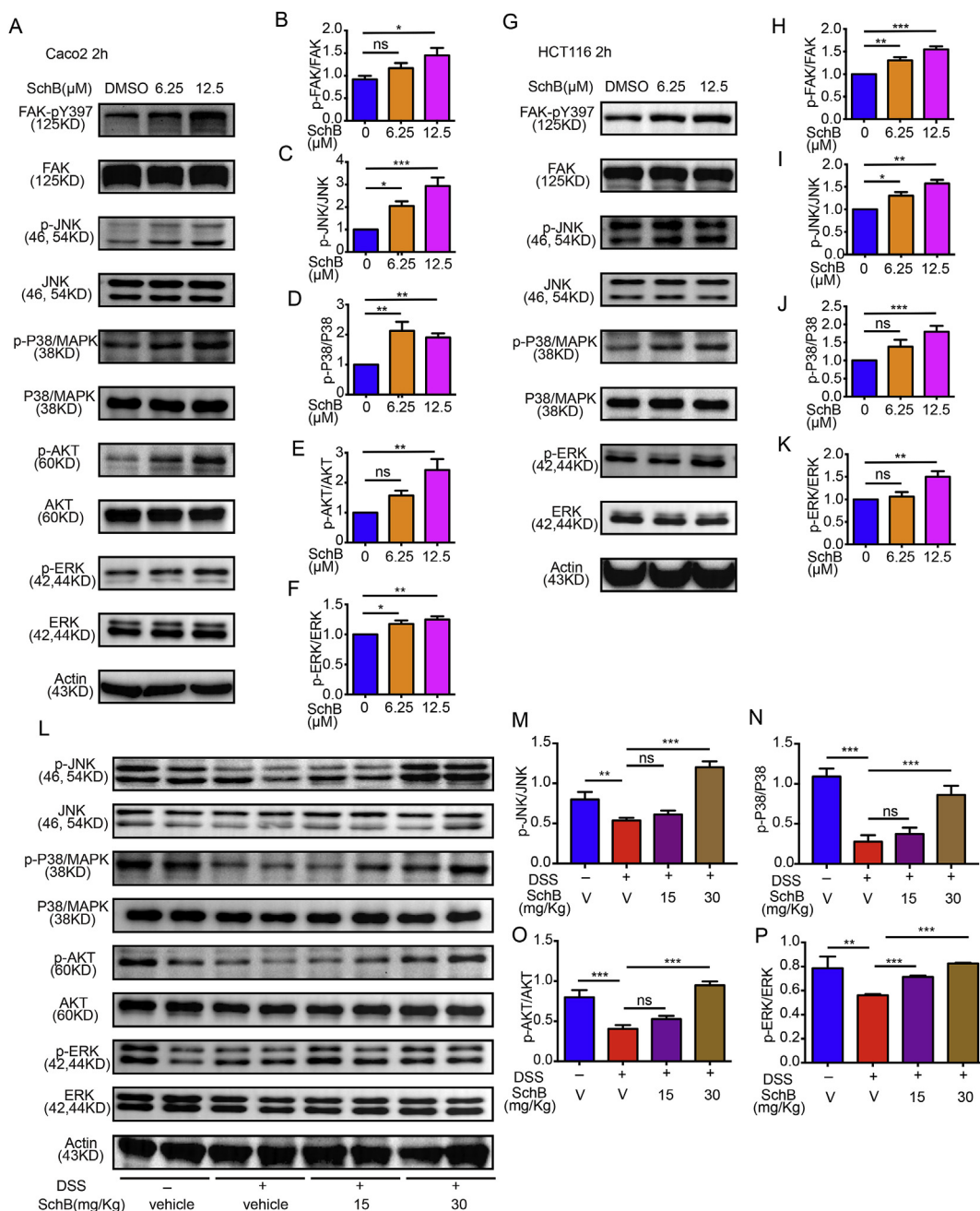


**Fig. 4. SchB stimulates activity of downstream signal of FAK both in vitro and vivo.** (A) Western Blot of typical kinases in FAK signaling, such as p-FAK (Py397), p-JNK (Thr183/Tyr185), p-P38/MAPK (Thr180/Tyr18), p-Akt (Ser473) and p-Erk (Thr202/Tyr204) in intestinal epithelial cell lines CACO2. (B–F) Quantification of western blot in Fig. 4A n = 6 in each group. 0 stands for DMSO. (G) Western Blot of typical kinases in FAK signaling, such as p-FAK (Py397), p-JNK (Thr183/Tyr185), p-P38/MAPK (Thr180/Tyr18) and p-Erk (Thr202/Tyr204) in intestinal epithelial cell lines HCT116. (H–K) Quantification of western blot in Fig. 4G n = 6 in each group. 0 stands for DMSO. (L) Western Blot of typical kinases downstream of FAK signaling, such as p-JNK (Thr183/Tyr185), p-P38/MAPK (Thr180/Tyr18), p-Akt (Ser473) and p-Erk (Thr202/Tyr204) in DSS-induced UC mice treated with SchB at indicated doses in the corresponding figure (0.5% CMC-Na for vehicle). (M–P) Quantification of western blot in Fig. 4L n = 6 in each group. V stands for Vehicle. Data were presented as the mean  $\pm$  S.E.M. \*P < 0.05, \*\*P < 0.01 and \*\*\*P < 0.001 vs. SchB (0  $\mu$ M) group.

was successful and that difference of gut microbiota caused by SchB treatment was neutralized by co-housing (Fig. 6M). Several pivotal OTUs, which was abundant in DSS-treated mice and disappeared when colitis mice were treated with SchB, still existed in SchB-treated colitis mice when these mice were co-housed with those colitis mice which received vehicle. These OTUs are OTU7 (Fig. 6N), OTU6 (Fig. 6O), OTU30 (Fig. 6P), OTU65 (Fig. 6Q) and OTU35 (Fig. 6R). These data indicated that SchB influenced gut microbiota, which was indispensable for protecting colon from DSS-induced damage, for microbiota transmission counteracted protective effect of SchB.

### 3.6. SchB potently inhibits initiation and promotion of CAC due to its alleviation of UC

Next, we tested if SchB prevented CAC because of its mitigation of UC. AOM/DSS mice model is a highly reliable and widely accepted model for CAC (Neufert et al., 2007) and DSS-induced UC is essential for CAC initiation and progression. We used this animal model in order to test if SchB can relieve CAC. We constructed the experiments as showed in (Fig. 7A). We found that SchB could significantly promote survival of AOM/DSS mice model, both at 15 mg/kg and 30 mg/kg

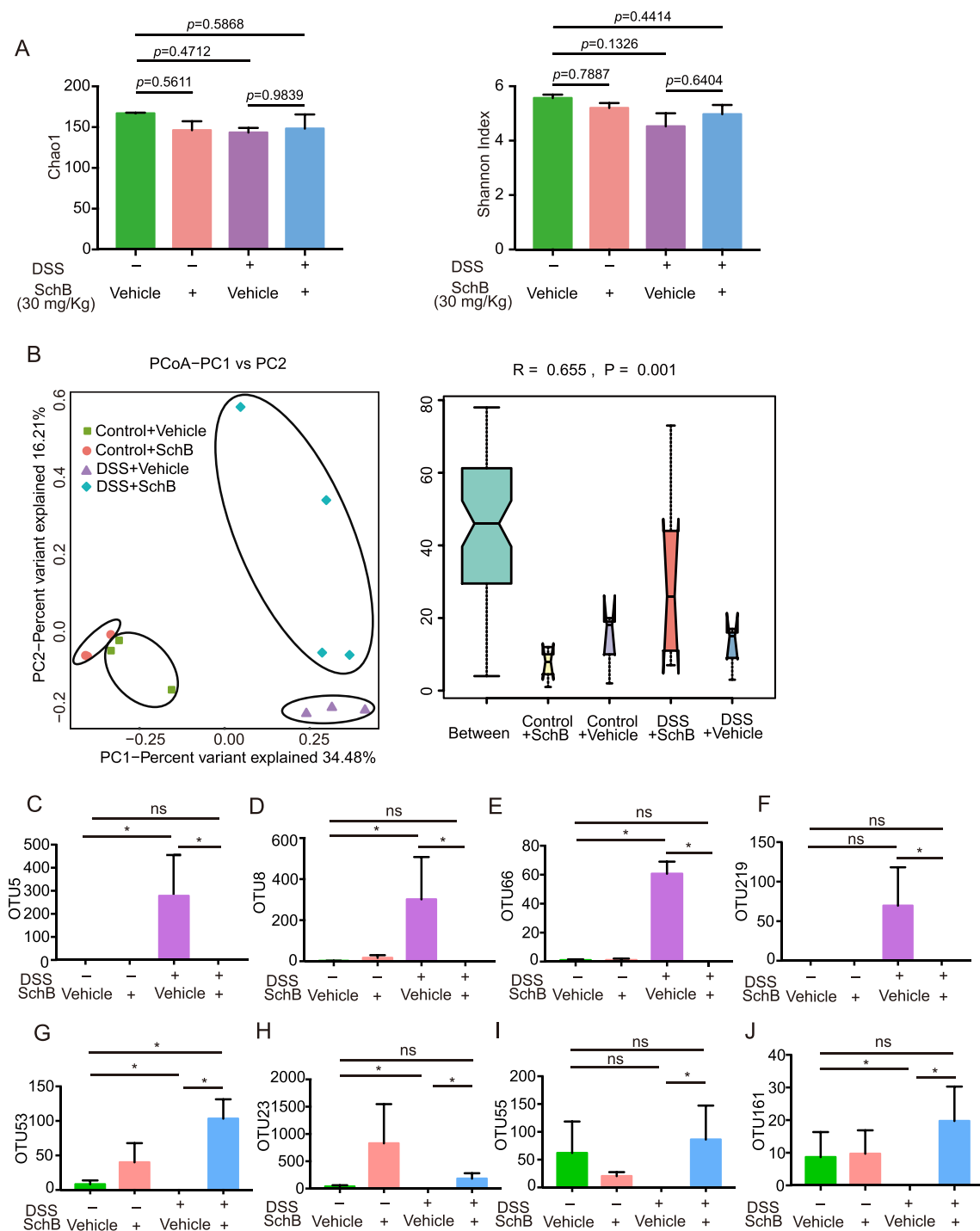


**Fig. 5. SchB influences gut microbiota.** (A) α Diversity of gut microbiota for mice in Control + vehicle (n = 3), Control + SchB (30 mg/kg) (n = 3), DSS + vehicle (n = 3) and DSS + SchB (30 mg/kg) (n = 4) groups. (B) PCoA and ANOSIM analysis of gut microbiota for mice in Control + vehicle, Control + SchB (30 mg/kg), DSS + vehicle and DSS + SchB (30 mg/kg) groups. (C–J) Absolute abundance of different OTUs in gut microbiota of mice in Control + vehicle, Control + SchB (30 mg/kg), DSS + vehicle and DSS + SchB (30 mg/kg) groups. Annotation for OTUs: OTU5 (related to Rhodospirillaceae); OTU8 (related to Mollicutes); OTU66 (related to *Gastranaerophilales*); OTU219 (related to *Lachnospiraceae*); OTU53 (related to *Bacteroides*); OTU23 (related to *Rikenellaceae RC9 gut group*); OTU55 (related to *Odoribacter laneus YIT 12061*); OTU161 (related to *coprostanoligenes*). Data were presented as the mean ± S.E.M. \*P < 0.05, \*\*P < 0.01, \*\*\*P < 0.001 vs. Control + Vehicle group or DSS + Vehicle group.

dosage (Fig. 7B). We repeated the experiment and killed the mice on day 63. Notably, SchB diminished tumor burden (Fig. 7C and D) and increased body weight of AOM/DSS mice model (Fig. 7E), which demonstrated that SchB could inhibit initiation and promotion of CAC in mice and improve survival of the AOM/DSS mice model due to its alleviation of UC. The mRNA and protein levels of mIL-6, TNF-α and mIL-

1β decreased in the colon of mice in AOM/DSS + SchB (15 mg/kg) and AOM/DSS + SchB (30 mg/kg) groups compared to those in AOM/DSS + vehicle group (Fig. 7F–K). These results indicated that SchB potently inhibits initiation and promotion of CAC and decreases production of inflammatory cytokines.

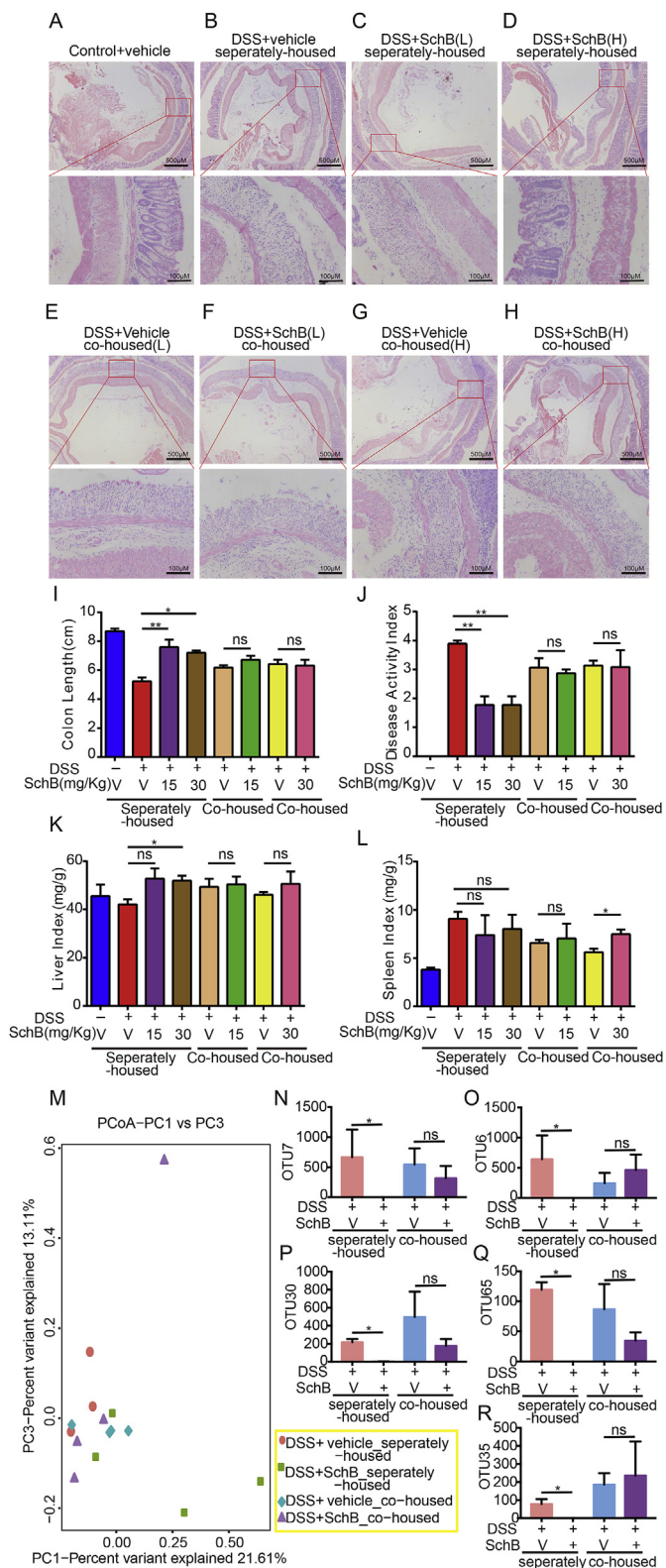


**Fig. 6. Microbiota transmission reverses the protection of colon of SchB.** n = 10 in Control + vehicle (separately housed), DSS + vehicle (separately housed), DSS + SchB (L) (separately housed), DSS + SchB (H) (separately housed) groups. n = 5 in DSS + vehicle co-housed (L), DSS + SchB (L) co-housed, DSS + vehicle co-housed (H) and DSS + SchB (H) co-housed groups. (A–H) H&E staining of colons of mice. L stands for low dose, 15 mg/kg. H stands for high dose, 30 mg/kg. Vehicle was 0.5% CMC-Na. DSS + vehicle co-housed (L): mice treated with DSS and vehicle (CMC-Na) and co housed with mice treated with DSS and SchB (15 mg/kg). DSS + SchB (L) co-housed: mice treated with DSS and SchB (15 mg/kg) and co housed with mice treated with DSS and vehicle (0.5% CMC-Na). DSS + vehicle co-housed (H): mice treated with DSS and vehicle (0.5% CMC-Na) and co housed with mice treated with DSS and SchB (30 mg/kg). DSS + SchB (H) co-housed: mice treated with DSS and SchB (30 mg/kg) and co housed with mice treated with DSS and vehicle (CMC-Na). Scale bars, 500  $\mu$ M for upper lines and 100  $\mu$ M for lower lines. (I–L) Colon lengths, Disease activity index, liver index and spleen index of mice. V stands for vehicle. (M) PCoA analysis of gut microbiota for mice separately-housed or co-housed. (N–R) Absolute abundance of different OTUs in gut microbiota of mice separately-housed or co-housed. V stands for vehicle. Annotation for OTUs: OTU7 (related to *Anaeroplasma*), OTU6 (related to *Rhodospirillaceae*); OTU30 (related to *Clostridiales\_vadinBB60\_group*); OTU65 (related to *Gastranaerophiles*) and OTU35 (related to *Clostridiales*). Groups are as shown in figures. Data were presented as the mean  $\pm$  S.E.M. \*P < 0.05, \*\*P < 0.01, \*\*\*P < 0.001 vs. Control + Vehicle group or DSS + Vehicle group. Scale bars are showed in figures.

numerous patients becoming intolerant or refractory to these available treatments (Vermeire et al., 2017). New options for treatments of ulcerative colitis are needed for the patients who could not benefit from treatments that already exist.

An efficient treatment that can prevent the progression of IBD and prevent CAC initiation is imperative. Here, we demonstrated that SchB significantly mitigated DSS-induced colitis. Comprehensive results showed that SchB potently alleviated colitis in mice. Although several previous studies have suggested that SchB inhibited inflammatory cytokines release in vitro, little is known if SchB exhibits immune suppressive effect in colitis. Our results showed that although SchB protected distal colon from DSS-induced damage, it failed to significantly inhibit some typical cytokines secretion such as IL-6 and TNF- $\alpha$  induced by LPS in both BMDM cells and iBMDM cell line. Furthermore, SchB was unsuccessful to improve survival of mice with LPS-induced sepsis. These data indicated that SchB could not suppress innate immune cells, at least in a direct way.

UC is a multifactor malady that involved interaction among intestinal epithelium, immune response and gut microbiota. Later we suggested that SchB protected intestinal epithelium integrity by activating FAK and this activity was essential, which was proved by the fact that PF562271 could reverse the effect of SchB. Moreover, western blot analysis revealed that SchB facilitated phosphorylation of FAK (p-Y397) and downstream signal of p-JNK, p-p38 MAPK, p-Akt and P-Erk, both in epithelium cell lines (CACO2 and HCT116) and in vivo. However, the underlying mechanism of how SchB activated FAK remains elusive. Further investigation needs to be conducted to figure out which molecule, FAK or other upstream proteins, SchB directly interact with and the precise action mode. Moreover, we could not exclude the possibility that SchB activated FAK by regulating other signal pathways. Our finding is controversial to some previous reports, which depended on the animal models and specific steps in tumor progression (Sulzmaier et al., 2014). Jong et al. have demonstrated that activating FAK signal pathway in macrophages enhanced the cells to infiltrate into tumors, which promoted CAC development (Woo et al., 2016). Heffler et al. demonstrated that FAK autophosphorylation inhibition decreased colon cancer cell growth and enhanced the efficacy of chemotherapy (Heffler et al., 2013). These researches all focus on cancer progression rather than initiation. Cancer is a complicated and multifactorial disease in which one molecule can play different roles in various steps of disease development. Our results indicated that activation of FAK in UC was

#### 4. Discussion

CAC is a worldwide malignancy that causes severe deaths, which develops from IBD within several years. Although many drugs for different targets are accessible for treatment of ulcerative colitis, such as 5-aminosalicylic acid, thiopurines and corticosteroids, there are still

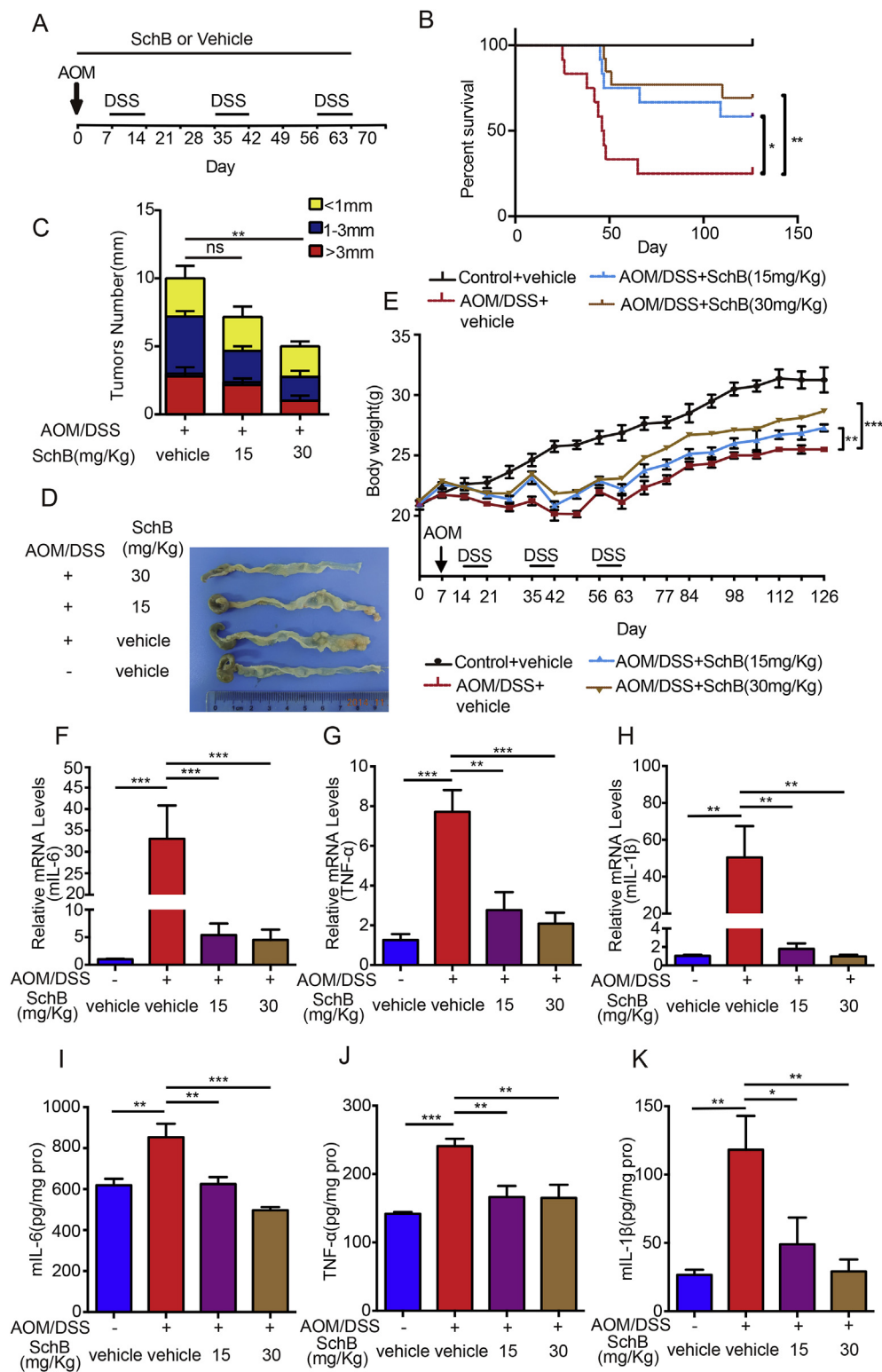


**Fig. 7.** SchB significantly prevented initiation and progression of CAC. For AOM/DSS model, the groups are as follows: Control + vehicle, AOM/DSS + vehicle, AOM/DSS + SchB (15 mg/kg), AOM/DSS + SchB (30 mg/kg). Vehicle was 0.5% CMC-Na. Dosage of AOM was 10 mg/kg and concentration of DSS was 2.5% (w/v) in drinking water, n = 12 or 13 in each group. (A) Procedure of AOM/DSS model induction and SchB treatment. (B) Survival curve, (C) Tumor burden, (D) Photo of colons, (E) Body weight of the AOM/DSS model treated with SchB at indicated doses in the corresponding figure (0.5% CMC-Na). (F–H) Relative mRNA levels of mice colon. Fig. 7F for mouse IL-6 (mIL-6), 7G for TNF- $\alpha$ , and 7H for mouse IL-1 $\beta$  (mIL-1 $\beta$ ). (I–K) ELISA assessing for cytokines levels in colons. Fig. 7I for mouse IL-6 (mIL-6), 7J for TNF- $\alpha$ , and 7K for mouse IL-1 $\beta$  (mIL-1 $\beta$ ). Data were presented as the mean  $\pm$  S.E.M. \*P < 0.05, \*\*P < 0.01, \*\*\*P < 0.001 vs. AOM/DSS + vehicle group or DSS + vehicle group.

efficient in protecting intestine epithelial barrier and inhibiting CAC initiation.

There is increasing evidence verifying that microbiota-host interaction plays an important role in many diseases including UC and it is a reliable way to alleviate UC severity by regulating microbiota (Garrett, 2015). In this study, we reported that efficiency of SchB partly relied on gut microbiota. It is well known that a specific species does not significantly change gut microbiota function and keeping balance of gut microbiota composition is essential to stay equilibrium of colon

microenvironment. We selected changes of some OTUs which are closely related to inflammatory disease to reflect profile of gut-microbiota. Transmission of gut microbiota by co-housing significantly reversed colon protection effect of SchB. 16S rRNA sequencing also pointed out that SchB adjusted eubiosis of gut-microbiota. These data innovatively uncovered the relationship between the preventative effect of SchB on colon and gut microbiota.

It is suggested that SchB is multifunctional drug. It has been reported that SchB efficiently ameliorated non-alcoholic fatty-liver

disease (NAFLD) by regulating multiple enzyme, such as fatty acid synthase and nuclear factor-erythroid-2-related factor-2, in lipid metabolic process (Kwan et al., 2015). It can ameliorate inflammation-associated disorder (Checker et al., 2012; Kwan et al., 2015; Lam and Ko, 2012; Li et al., 2006, 2007; Nishida et al., 2009; Pan et al., 2006; Qiangrong et al., 2005; Sun et al., 2007; Zhang et al., 2013). Previous studies have strongly demonstrated the anti-inflammation and anti-oxidative stress effects of SchB (Checker et al., 2012; Kwan et al., 2015) through activation of NADPH oxidase 4 (NOX4) or Nrf2. Furthermore, some articles have also reported that SchB was a dual inhibitor of both P-glycoprotein (P-gp) and multidrug resistance-associated protein 1 (MRP1), which potently prevents doxorubicin-induced cardiotoxicity via enhancing glutathione redox cycling (Pan et al., 2006; Qiangrong et al., 2005). A previous study has demonstrated the detailed pharmacokinetic characteristics of SchB (Wang et al., 2018). Briefly, after oral administration, the values of  $C_{max}$  (the maximum concentration) were 85.8, 251.8 and 612.0 ng/ml for male rats at 10, 20 and 40 mg/kg, respectively. The dose-normalized  $AUC_{0-t}$  (Area under concentration-time curve) values were 513.8, 1471.6 and 3852.0 ng·ml for male rats for SchB at 10, 20 and 40 mg/kg, respectively, indicating that the pharmacokinetic process of SchB was consistent with dose-proportional pharmacokinetics in male rats. The  $t_{max}$  (time at which  $C_{max}$  was achieved) and  $t_{1/2}$  (elimination half-time) of SchB ranged from 5.0 to 7.8 h and from 3.3 to 7.0 h following oral administration, suggesting a slow absorption of SchB into systemic circulation and then slow clearance from the rat plasma. As for tissue distribution, SchB could be detected in various tissues, including small and large intestine. SchB in most tissues reached peak level at 2 h after oral administration. The highest concentrations of SchB were detected in the ovary, followed by the adipose tissue, which is possibly due to the lipid-soluble properties and small molecular weight. The main excretion route of SchB was via feces. Although the underlying mechanism of how DSS caused UC remains largely unknown, it has been reported that DSS inhibited DNA duplication and increased epithelium apoptosis possibly due to strong negative charge of DSS (Chassaing et al., 2014). SchB is lipid-soluble and hardly dissolved in water at all. Therefore, it is reasonable that SchB would rather have effect on colons than directly interact with DSS which is highly water dissolved, especially *in vivo*.

Innovatively, our results uncovered new pharmacology effect of SchB on relieving AOM/DSS-induced CAC and DSS-induced colitis. It has been reported that mitigating colitis can strongly prevent initiation of CAC (Terzic et al., 2010). We found that SchB did almost no harm to normal colons and mice so it has little side effect.

Taken together, our results suggested that SchB exhibited significantly efficiency to prevent initiation and development of CAC and UC, which is potential to be developed to an effective treatment for UC and prevention of CAC.

## 5. Conclusion

We reported for the first time that SchB was potent to inhibit CAC and UC in mice. FAK activation by SchB was indispensable for protective effect on DSS-induced colitis. The protective efficiency of SchB also relied on gut microbiota. We found a natural compound which potentially becomes a new prevention and treatment of CAC and UC. The protection mechanisms of SchB broaden our horizon that natural products and multi-target treatments may benefit to UC patients.

## Conflicts of interest

All authors confirm that there are no known conflicts of interest associated with this publication.

## Acknowledgements

JL designed and performed the study and wrote the paper. Yuan Lu,

DW, FQ and XC analyzed the data. RS, SZ, WT, DD, XG, QC, DZ, RQ, ZY, LH, KH and CC performed the study. YY and ZC designed the study and critically revised the manuscript. Yan Luo critically revised the manuscript. All authors have approved the final article should be true and included in the disclosure.

This work was supported by the National Natural Science Foundation of China [Nos. 81673468, 91529304, 81473230, 81273547, 81403020, 91129731 to YY, 81672752 to ZC and 81603132 to XG], the Natural Science Foundation of Jiangsu Province [No. BK20170739 to Yan Luo], the Project Program of State Key Laboratory of Natural Medicines, China Pharmaceutical University (No. SKLNMZZCX201609), the Research of Natural Science in Colleges and Universities in Jiangsu Province [17KJD310002 to CC] and the 111 Project [No111-2-07].

## Appendix A. Supplementary data

Supplementary data to this article can be found online at <https://doi.org/10.1016/j.ejphar.2019.03.059>.

## References

- Ashton, G.H., Morton, J.P., Myant, K., Phesse, T.J., Ridgway, R.A., Marsh, V., Wilkins, J.A., Athineos, D., Muncan, V., Kemp, R., Neufeld, K., Clevers, H., Brunton, V., Winton, D.J., Wang, X., Sears, R.C., Clarke, A.R., Frame, M.C., Sansom, O.J., 2010. Focal adhesion kinase is required for intestinal regeneration and tumorigenesis downstream of Wnt/c-Myc signaling. *Dev. Cell* 19, 259–269.
- Caporaso, J.G., Lauber, C.L., Walters, W.A., Berg-Lyons, D., Lozupone, C.A., Turnbaugh, P.J., Fierer, N., Knight, R., 2011. Global patterns of 16S rRNA diversity at a depth of millions of sequences per sample. *Proc. Natl. Acad. Sci. U. S. A.* 108 (Suppl. 1), 4516–4522.
- Chassaing, B., Aitken, J.D., Malleshappa, M., Vijay-Kumar, M., 2014. Dextran sulfate sodium (DSS)-induced colitis in mice. *Curr. Protoc. Im.* 104 Unit 15 25.
- Chassaing, B., Koren, O., Goodrich, J.K., Poole, A.C., Srinivasan, S., Ley, R.E., Gewirtz, A.T., 2015. Dietary emulsifiers impact the mouse gut microbiota promoting colitis and metabolic syndrome. *Nature* 519, 92–96.
- Checker, R., Patwardhan, R.S., Sharma, D., Menon, J., Thoh, M., Bhilwade, H.N., Konishi, T., Sandur, S.K., 2012. Schisandrin B exhibits anti-inflammatory activity through modulation of the redox-sensitive transcription factors Nrf2 and NF- $\kappa$ B. *Free Radic. Biol. Med.* 53, 1421–1430.
- Chen, J., Wang, H., Long, W., Shen, X., Wu, D., Song, S.S., Sun, Y.M., Liu, P.X., Fan, S., Fan, F., Zhang, X.D., 2013. Sex differences in the toxicity of polyethylene glycol-coated gold nanoparticles in mice. *Int. J. Nanomed.* 8, 2409–2419.
- Chiari, T.R., Soto, R., Zac Stephens, W., Kubinak, J.L., Petersen, C., Gogokhia, L., Bell, R., Delgado, J.C., Cox, J., Voth, W., Brown, J., Stillman, D.J., O'Connell, R.M., Tebo, A.E., Round, J.L., 2017. A member of the gut mycobiota modulates host purine metabolism exacerbating colitis in mice. *Sci. Transl. Med.* 9.
- Chu, H., Khosravi, A., Kusumawardhani, I.P., Kwon, A.H., Vasconcelos, A.C., Cunha, L.D., Mayer, A.E., Shen, Y., Wu, W.L., Kambal, A., Targan, S.R., Xavier, R.J., Ernst, P.B., Green, D.R., McGovern, D.P., Virgin, H.W., Mazmanian, S.K., 2016. Gene-microbiota interactions contribute to the pathogenesis of inflammatory bowel disease. *Science* 352, 1116–1120.
- Cui, S., Wang, J., Wu, Q., Qian, J., Yang, C., Bo, P., 2017. Genistein inhibits the growth and regulates the migration and invasion abilities of melanoma cells via the FAK/paxillin and MAPK pathways. *Oncotarget* 8, 21674–21691.
- Forbes, J.D., Van Domselaar, G., Bernstein, C.N., 2016. The gut microbiota in immune-mediated inflammatory diseases. *Front. Microbiol.* 7, 1081.
- Gagniere, J., Raisch, J., Veziant, J., Barnich, N., Bonnet, R., Buc, E., Bringer, M.A., Pezet, D., Bonnet, M., 2016. Gut microbiota imbalance and colorectal cancer. *World J. Gastroenterol.* 22, 501–518.
- Gao, X., Cao, Q., Cheng, Y., Zhao, D., Wang, Z., Yang, H., Wu, Q., You, L., Wang, Y., Lin, Y., Li, X., Wang, Y., Bian, J.S., Sun, D., Kong, L., Birnbaumer, L., Yang, Y., 2018. Chronic stress promotes colitis by disturbing the gut microbiota and triggering immune system response. *Proc. Natl. Acad. Sci. U. S. A.* 115, E2960–E2969.
- Garrett, W.S., 2015. Cancer and the microbiota. *Science* 348, 80–87.
- Guo, S., Nighot, M., Al-Sadi, R., Alhmoud, T., Nighot, P., Ma, T.Y., 2015. Lipopolysaccharide regulation of intestinal tight junction permeability is mediated by TLR4 signal transduction pathway activation of FAK and MyD88. *J. Immunol.* 195, 4999–5010.
- Heffler, M., Golubovskaya, V.M., Dunn, K.M., Cance, W., 2013 Aug Aug. Focal adhesion kinase autoprophosphorylation inhibition decreases colon cancer cell growth and enhances the efficacy of chemotherapy. *Cancer Biol. Ther.* 14 (8), 761–772.
- Hudson, L.E., Anderson, S.E., Corbett, A.H., Lamb, T.J., 2017. Gleaning insights from fecal microbiota transplantation and probiotic studies for the rational design of combination microbial therapies. *Clin. Microbiol. Rev.* 30, 191–231.
- Ijsseennagger, N., Belzer, C., Hooiveld, G.J., Dekker, J., van Mil, S.W., Muller, M., Kleerebezem, M., van der Meer, R., 2015. Gut microbiota facilitates dietary heme-induced epithelial hyperproliferation by opening the mucus barrier in colon. *Proc. Natl. Acad. Sci. U. S. A.* 112, 10038–10043.

- Kwan, H.Y., Niu, X., Dai, W., Tong, T., Chao, X., Su, T., Chan, C.L., Lee, K.C., Fu, X., Yi, H., Yu, H., Li, T., Tse, A.K., Fong, W.F., Pan, S.Y., Lu, A., Yu, Z.L., 2015. Lipidomic-based investigation into the regulatory effect of Schisandrin B on palmitic acid level in non-alcoholic steatotic livers. *Sci. Rep.* 5, 9114.
- Laharie, D., 2017. Towards therapeutic choices in ulcerative colitis. *Lancet* 390, 98–99.
- Lam, P.Y., Ko, K.M., 2012. Schisandrin B as a hormetic agent for preventing age-related neurodegenerative diseases. *Oxidative medicine and cellular longevity* 2012, 250825.
- Leoni, G., Alam, A., Neumann, P.A., Lambeth, J.D., Cheng, G., McCoy, J., Hilgarth, R.S., Kundu, K., Murthy, N., Kusters, D., Reutelingsperger, C., Perretti, M., Parkos, C.A., Neish, A.S., Nusrat, A., 2013. Annexin A1, formyl peptide receptor, and NOX1 orchestrate epithelial repair. *J. Clin. Investig.* 123, 443–454.
- Li, L., Lu, Q., Shen, Y., Hu, X., 2006. Schisandrin B enhances doxorubicin-induced apoptosis of cancer cells but not normal cells. *Biochem. Pharmacol.* 71, 584–595.
- Li, L., Pan, Q., Han, W., Liu, Z., Hu, X., 2007. Schisandrin B prevents doxorubicin-induced cardiotoxicity via enhancing glutathione redox cycling. *Clin. Cancer Res. : an official journal of the American Association for Cancer Research* 13, 6753–6760.
- Murano, M., Maemura, K., Hirata, I., Toshina, K., Nishikawa, T., Hamamori, N., Sasaki, S., Saitoh, O., Katsu, K., 2000. Therapeutic effect of intracolonically administered nuclear factor kappa B (p65) antisense oligonucleotide on mouse dextran sulphate sodium (DSS)-induced colitis. *Clin. Exp. Immunol.* 120, 51–58.
- Na, Y.R., Hong, J.H., Lee, M.Y., Jung, J.H., Jung, D., Kim, Y.W., Son, D., Choi, M., Kim, K.P., Seok 2nd, S.H., 2015. Proteomic analysis reveals distinct metabolic differences between granulocyte-macrophage colony stimulating factor (GM-CSF) and macrophage colony stimulating factor (M-CSF) grown macrophages derived from murine bone marrow cells. *Mol. Cell. Proteomics* 14, 2722–2732.
- Nagalingam, N.A., Kao, J.Y., Young, V.B., 2011. Microbial ecology of the murine gut associated with the development of dextran sodium sulfate-induced colitis. *Inflamm. Bowel Dis.* 17, 917–926.
- Neufert, C., Becker, C., Neurath, M.F., 2007. An inducible mouse model of colon carcinogenesis for the analysis of sporadic and inflammation-driven tumor progression. *Nat. Protoc.* 2, 1998–2004.
- Nishida, H., Tatewaki, N., Nakajima, Y., Magara, T., Ko, K.M., Hamamori, Y., Konishi, T., 2009. Inhibition of ATR protein kinase activity by schisandrin B in DNA damage response. *Nucleic Acids Res.* 37, 5678–5689.
- Owen, J.L., Mohamadzadeh, M., 2013. Microbial activation of gut dendritic cells and the control of mucosal immunity. *J. Interferon Cytokine Res. : the official journal of the International Society for Interferon and Cytokine Research* 33, 619–631.
- Owen, K.A., Abshire, M.Y., Tilghman, R.W., Casanova, J.E., Bouton, A.H., 2011. FAK regulates intestinal epithelial cell survival and proliferation during mucosal wound healing. *PLoS One* 6, e23123.
- Pan, Q., Lu, Q., Zhang, K., Hu, X., 2006. Dibenzocyclooctadiene lignans: a class of novel inhibitors of P-glycoprotein. *Cancer Chemother. Pharmacol.* 58, 99–106.
- Qiangrong, P., Wang, T., Lu, Q., Hu, X., 2005. Schisandrin B-a novel inhibitor of P-glycoprotein. *Biochem. Biophys. Res. Commun.* 335, 406–411.
- Shi, H., Lin, B., Huang, Y., Wu, J., Zhang, H., Lin, C., Wang, Z., Zhu, J., Zhao, Y., Fu, X., Lou, Z., Li, X., Xiao, J., 2016. Basic fibroblast growth factor promotes melanocyte migration via activating PI3K/Akt-Rac1-FAK-JNK and ERK signaling pathways. *IUBMB Life* 68, 735–747.
- Siu, E.R., Wong, E.W., Mruk, D.D., Porto, C.S., Cheng, C.Y., 2009. Focal adhesion kinase is a blood-testis barrier regulator. *Proc. Natl. Acad. Sci. U. S. A.* 106, 9298–9303.
- Slater, T.W., Finkelsztejn, A., Mascarenhas, L.A., Mehl, L.C., Butin-Israeli, V., Sumagin, R., 2017. Neutrophil microparticles deliver active myeloperoxidase to injured mucosa to inhibit epithelial wound healing. *J. Immunol.* 198, 2886–2897.
- Sommer, J., Engelowski, E., Baran, P., Garbers, C., Floss, D.M., Scheller, J., 2014.
- Interleukin-6, but not the interleukin-6 receptor plays a role in recovery from dextran sodium sulfate-induced colitis. *Int. J. Mol. Med.* 34, 651–660.
- Su, L., Mruk, D.D., Lui, W.Y., Lee, W.M., Cheng, C.Y., 2011. P-glycoprotein regulates blood-testis barrier dynamics via its effects on the occludin/zonula occludens 1 (ZO-1) protein complex mediated by focal adhesion kinase (FAK). *Proc. Natl. Acad. Sci. U. S. A.* 108, 19623–19628.
- Sulzmaier, F.J., Jean, C., Schlaepfer, D.D., 2014. FAK in cancer: mechanistic findings and clinical applications. *Nat. Rev. Canc.* 14, 598–610.
- Sun, M., Xu, X., Lu, Q., Pan, Q., Hu, X., 2007. Schisandrin B: a dual inhibitor of P-glycoprotein and multidrug resistance-associated protein 1. *Cancer Lett.* 246, 300–307.
- Surana, N.K., Kasper, D.L., 2017. Moving beyond microbiome-wide associations to causal microbe identification. *Nature* 552, 244–247.
- Terzic, J., Grivennikov, S., Karin, E., Karin, M., 2010. Inflammation and colon cancer. *Gastroenterology* 138, 2101–2114 e2105.
- Tsoi, H., Chu, E.S.H., Zhang, X., Sheng, J., Nakatsu, G., Ng, S.C., Chan, A.W.H., Chan, F.K.L., Sung, J.J.Y., Yu, J., 2017. Peptostreptococcus anaerobius induces intracellular cholesterol biosynthesis in colon cells to induce proliferation and causes dysplasia in mice. *Gastroenterology* 152, 1419–1433 e1415.
- Ullman, T.A., Itzkowitz, S.H., 2011. Intestinal inflammation and cancer. *Gastroenterology* 140, 1807–1816.
- Ungaro, R., Mehandru, S., Allen, P.B., Peyrin-Biroulet, L., Colombel, J.-F., 2017. Ulcerative colitis. *Lancet* 389, 1756–1770.
- Vermeire, S., Sandborn, W.J., Danese, S., Hebuterne, X., Salzberg, B.A., Klopocka, M., Tarabar, D., Vanasek, T., Gregus, M., Hellstern, P.A., Kim, J.S., Sparrow, M.P., Gorelick, K.J., Hinz, M., Ahmad, A., Pradhan, V., Hassan-Zahraee, M., Clare, R., Cataldi, F., Reinisch, W., 2017. Anti-MADCAM antibody (PF-00547659) for ulcerative colitis (TURANDOT): a phase 2, randomised, double-blind, placebo-controlled trial. *Lancet* 390, 135–144.
- Wang, L., Chiang, E.T., Simmons, J.T., Garcia, J.G., Dudek, S.M., 2011. FTY720-induced human pulmonary endothelial barrier enhancement is mediated by c-Abl. *Eur. Respir. J.* 38, 78–88.
- Wang, Z., You, L., Cheng, Y., Hu, K., Wang, Z., Cheng, Y., Yang, J., Yang, Y., Wang, G., 2018. Investigation of pharmacokinetics, tissue distribution and excretion of schisandrin B in rats by HPLC-MS/MS. *Biomed. Chromatogr.* 32.
- Weischenfeldt, J., Porse, B., 2008. Bone Marrow-Derived Macrophages (BMM): Isolation and Applications. *CSH Protoc.* 2008. pdm prot5080.
- Woo, J.K., Jang, Y.S., Kang, J.H., Hwang, J.I., Seong, J.K., Lee, S.J., Jeon, S., Oh, G.T., Lee, H.Y., Oh, S.H., 2016. Ninjurin1 inhibits colitis-mediated colon cancer development and growth by suppression of macrophage infiltration through repression of FAK signaling. *Oncotarget* 7, 29592–29604.
- Yamada, K., Green, K.G., Samarel, A.M., Saffitz, J.E., 2005. Distinct pathways regulate expression of cardiac electrical and mechanical junction proteins in response to stretch. *Circ. Res.* 97, 346–353.
- Yamamoto, M., Matsumoto, S., 2016. Gut microbiota and colorectal cancer. *Genes Environ.* 38, 11.
- Yang, T., Owen, J.L., Lightfoot, Y.L., Kladde, M.P., Mohamadzadeh, M., 2013. Microbiota impact on the epigenetic regulation of colorectal cancer. *Trends Mol. Med.* 19, 714–725.
- Zeuner, A., Todaro, M., Stassi, G., De Maria, R., 2014. Colorectal cancer stem cells: from the crypt to the clinic. *Cell Stem Cell* 15, 692–705.
- Zhang, B., Liu, Z., Hu, X., 2013. Inhibiting cancer metastasis via targeting NAPDH oxidase 4. *Biochem. Pharmacol.* 86, 253–266.
- Zheng, P., Ji, G., Ma, Z., Liu, T., Xin, L., Wu, H., Liang, X., Liu, J., 2009. Therapeutic effect of puerarin on non-alcoholic rat fatty liver by improving leptin signal transduction through JAK2/STAT3 pathways. *Am. J. Chin. Med.* 37, 69–83.